Piezofluorochromism in Covalent Organic Frameworks: Pressure-induced Emission Enhancement and Blue-Shifted Emission

Jing Fang,[†][a] Xihan Yu,[†][b] Yaozu Liu,*[a] Yusran Yusran,[a] Yujie Wang,[a] Valentin Valtchev,[a] Shilun Qiu,[a] Bo Zou,*[b] and Qianrong Fang*[a]

[a] J. Fang, Dr. Y. Liu, Dr. Y. Yusran, Dr. Y. Wang, Prof. S. Qiu and Prof. Q. Fang
State Key Laboratory of Inorganic Synthesis and Preparative Chemistry, Department of Chemistry
Jilin University, Changchun 130012, China
E-mail: yaozuliu@jlu.edu.cn; qrfang@jlu.edu.cn

[b] X. Yu and Prof. B. Zou
State Key Laboratory of Superhard Materials, College of Physics
Jilin University, Changchun 130012, P. R. China
E-mail: zoubo@jlu.edu.cn

[c] Prof. V. Valtchev
Qingdao Institute of Bioenergy and Bioprocess Technology, Chinese Academy of Sciences, 189 Songling Road, Qingdao 266101, P. R. China
Normandie Univ, ENSICAEN, UNICAEN, CNRS, Laboratoire Catalyse et Spectrochimie, 6 Marechal Juin, 14050 Caen, France

[†] These authors contributed equally to this work.

Supporting information for this article is given via a link at the end of the document.

Abstract: Achieving enhanced or blue-shifted emission from piezochromic materials remains a major challenge. Covalent organic frameworks (COFs) are promising candidates for the development of piezochromic materials owing to their dynamic structures and adjustable optical properties, where the emission behaviors are not solely determined by the functional groups, but are also greatly influenced by the specific geometric arrangement. Nevertheless, this area remains relatively understudied. In this study, a successful synthesis of a series of bicarbazole-based COFs with varying topologies, dimensions, and linkages was conducted, followed by an investigation of their structural and emission properties under hydrostatic pressure generated by a diamond anvil cell. Consequently, these COFs exhibited distinct piezochromic behaviors, particularly a remarkable pressure-induced emission enhancement (PIEE) phenomenon with a 16-fold increase in fluorescence intensity from three-dimensional COFs, surpassing the performance of CPMs and most organic small molecules with PIEE behavior. On the contrary, three two-dimensional COFs with flexible structures exhibited rare blue-shifted emission, whereas the variants with rigid and conjugated structures showed common red-shifted and reduced emission. Mechanism research further revealed that these different piezochromic behaviors were primarily determined by interlayer distance and interaction. This study represents the first systematic exploration of the structures and emission properties of COFs through pressure-treated engineering and provides a new perspective on the design of piezochromic materials.

Introduction

Leveraging pressure-treated engineering is crucial for manipulating the structural and optical characteristics of materials, particularly in the development of piezochromic luminescent materials.[1] These pressure-responsive materials, which exhibit multi-color switching in response to external stimuli such as pressing, shearing, and grinding, have garnered significant attention for their potential applications in advanced photonics, pressure sensing, data storage, and memory devices.[2] Especially under the isotropic hydrostatic pressure from a diamond anvil cell (DAC), piezochromic materials, including organic compounds,[3] perovskites[4] and metal complexes,[5] exhibiting outstanding pressure-responsive performance, such as pressure-induced emission enhancement (PIEE),[6] blue-shifted emission,[7] white-light emitting.[8] However, owing to the formation of a low-energy emission species and a nonradiative “dark” state (e.g., narrow-bandgap excimer), most luminescent materials show a gradual red-shifted and quenched emission as pressure increases.[9] The amount of blue shift and/or magnitude of luminescence enhancement remain limited and a universal mechanism to design such piezochromic luminescent materials remains lacking.[10] Investigating novel materials with pressure-sensitive capabilities, demonstrating distinct pressure-dependent functionalities, and elucidating structure-property correlations are pivotal for advancing this domain.

Scheme 1. Illustration of design of seven bicarbazole-based COFs with different dimensions, topologies, and linkages for studying piezochromic effects under DAC.

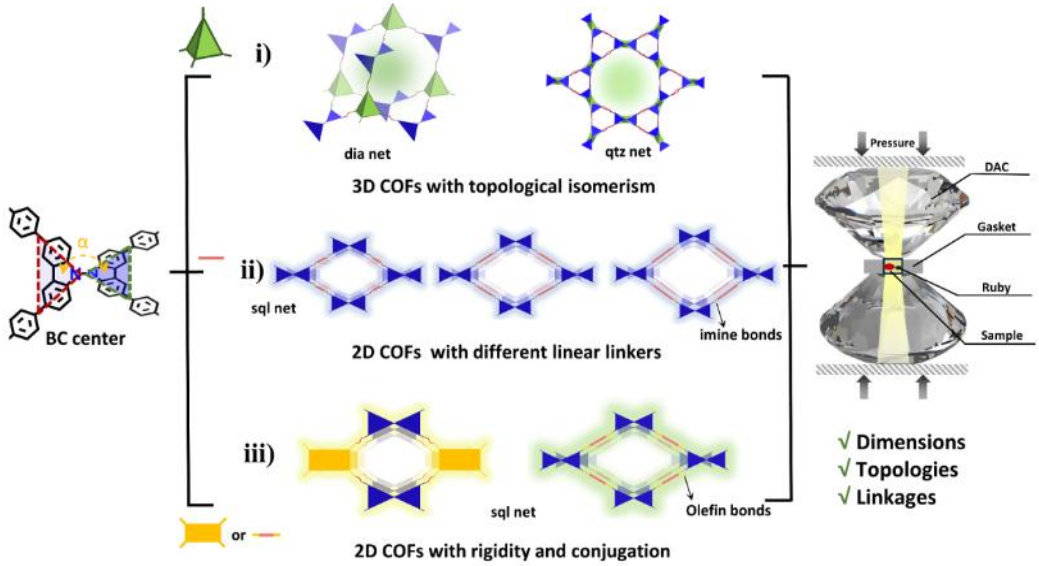

Covalent organic frameworks (COFs) are an emerging type of crystalline porous materials (CPMs) consisting of interconnected multi-functional organic building blocks featuring predesignable and periodic frameworks.[11] The optical properties of COFs are not solely determined by the functional groups within the structure, but are also greatly influenced by the specific geometric arrangement.[12] It is well-established that pressure plays a crucial role in enhancing molecular accumulation, controlling intermolecular interactions, and modifying molecular conformation.[13] Consequently, pressure serves as a powerful and environmentally friendly tool for regulating the structures and optical properties of COFs. Nevertheless, research on piezochromic COFs is still in the early stage. Our previous research has demonstrated that three-dimensional (3D) COFs exhibit remarkable variations in emission, high sensitivity, and excellent reversibility in response to hydrostatic pressure applied by DAC.[14] These findings support the hypothesis that functional groups positively impact the emission properties of COFs. In addition to functional groups, we are interested in investigating the influence of other parameters, such as connection, orientation, and alignment of the molecular building blocks, on the optical properties of COF materials. We aim to determine whether pressure can modulate these factors and induce unique pressure-responsive behavior without solely relying on functional groups which will be of importance to guide COF design and shed light on the relationship between structure/packing and corresponding piezochromic behavior. Moreover, the building blocks in COFs are interconnected to form extended and crystalline networks, with the connectivity determined by both the linkage and the shape of the building blocks. This characteristic allows for a wide range of possible topologies in COF design. Notably, building blocks with a twisted geometry, such as N,N'-bicarbazole (BC) where two carbazole planes form a significant dihedral angle along the rotatable N-N bond, have been found to generate different topologies in 3D COFs and weaken interlayer π–π packing in two-dimensional (2D) COFs.[15] Leveraging this observation, we expect the piezochromic behavior of bicarbazole-based COFs to show significant variations, guiding the design for piezochromic COFs.

Herein, a series of 2D and 3D bicarbazole-based COFs were successfully synthesized using the BC center, resulting in COFs with diverse dimensions, topologies, and linkages. The assembled COFs can be categorized as follows (Scheme 1): (i) Condensation of the BC center with tetrahedral linkers produced two isomeric 3D COFs with **dia** or **qtz** nets. (ii) Condensation of the BC center with linear linkers resulted in three 2D COFs with flexible skeletons. (iii) Condensation of the BC center with 2D linkers, incorporating increased rigidity and conjugation, led to two 2D COFs with enhanced π-π interactions between layers. These seven COFs were then subjected to piezochromic behavior studies using a DAC technique. Remarkably, both 3D COFs exhibited a remarkable PIEE phenomenon under hydrostatic pressure, where the fluorescence intensity increased by a factor of 16, surpassing the performance of CPMs and most organic small molecules with PIEE behavior known thus far. Among the three 2D COFs with linear linkers, an extraordinary blue-shift in the emission wavelength was observed, which is relatively rare within the field of piezochromism. Additionally, the last group of COFs exhibited red-shifted fluorescence emission and a gradual decrease in intensity, distinguishing them from the flexible 2D COFs. Subsequently, mechanism research revealed that the differences in piezochromism observed in these bicarbazole-based COFs can be attributed to the interlayer distance and interactions. This study provides an approach to regulate the emission performance of COFs, offering valuable insights for further advancements in this field.

Results and Discussion

These bicarbazole-linked COFs were synthesized using the solvothermal method by copolymerizing a derivative of bicarbazole containing aldehyde groups, known as 4,4',4'',4'''-([9,9'-bicarbazole]-3,3',6,6'-tetrayl)tetr-benzaldehyde (BCTB-4CHO), with tetramines, various aromatic amines, and 1,4-phenylenediacetonitrile (PDAN). The synthetic process and experimental details can be found in the Supporting Information, Experimental Section. As a result, different COFs with distinct

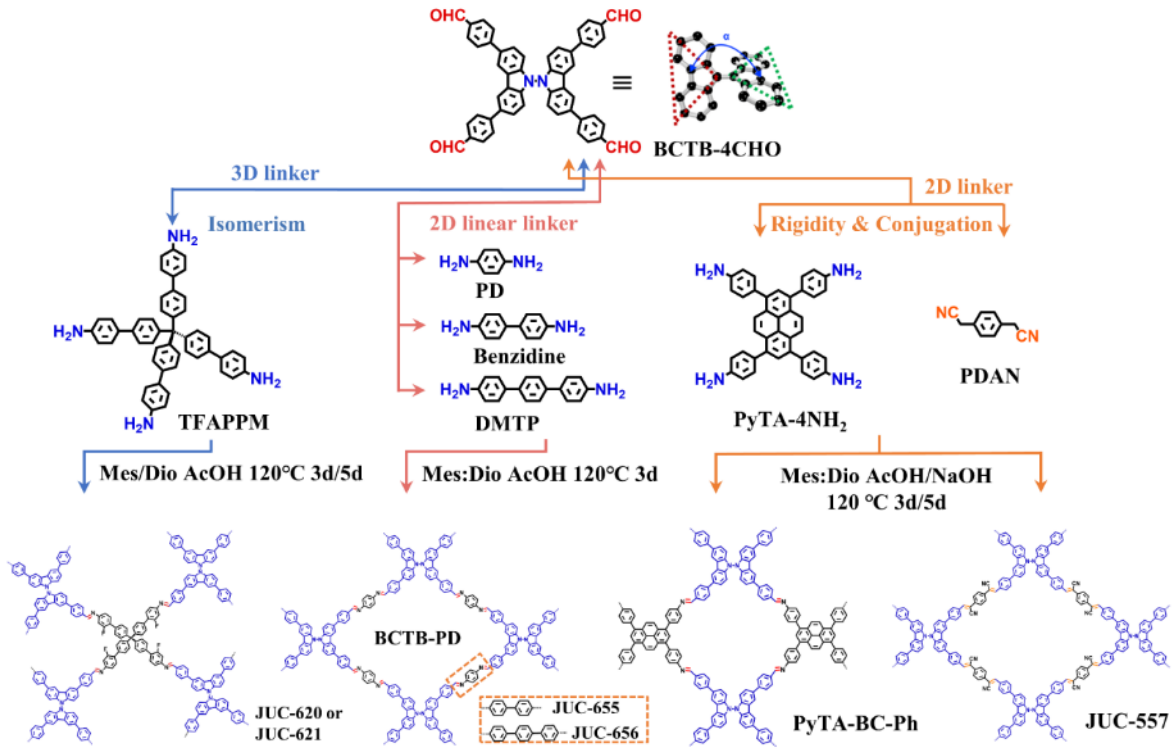

Figure 1. Condensation of BCTB-4CHO with different linkers to produce the seven COFs, corresponding to the three categories respectively.

topologies, dimensions, and linkages were obtained, as depicted in Figure 1. Notably, we successfully synthesized topological isomers of 3D COFs, namely JUC-620 with a **dia** net and JUC-621 with a **qtz** net, by polymerizing BCTB-4CHO with tetra[(2-fluoro-4-aminophenyl)phenyl]methane (TFAPPM) under different conditions (5 days in a solution of 1,3,5-mesitylene or 3 days in 1,4-dioxane).[15a] Furthermore, by altering the linker of linear aromatic diamines, such as *p*-phenylenediamine (PD), benzidine, and 4,4'-diaminoterphenyl (DMTP), we obtained three flexible 2D COFs, namely BCTB-PD,[16] as well as newly synthesized JUC-655 and JUC-656. Additionally, the poly-condensation of 4,4',4'',4'''-pyrene-1,3,6,8-tetrayl) tetraaniline (PyTA-4NH_2) and PDAN with BCTB-4CHO resulted in the formation of PyTA-BC-Ph[17] and JUC-557,[18] featuring π-stacked architectures or sp^2 C=C linkages. These variations in synthesis provide a wider range of options in terms of rigidity and conjugation for comparison.

The morphology of the as-prepared COFs was investigated using scanning electron microscopy (SEM) and transmission electron microscopy (TEM), revealing the uniform structure (Figures S1-S7). The samples underwent analysis using various spectroscopic techniques. The Fourier-transformed infrared (FT-IR) spectra indicated the presence of characteristic imine (C=N) stretching bands within the range of 1621-1626 cm^{-1}, confirming the formation of imine linkages (Figures S8-S10). The FT-IR spectrum of JUC-557 in particular revealed the formation of sp^2 carbon-conjugated COF structure, as evident from the appearance of a new C≡N vibration band at 2221 cm^{-1} (Figure S10b). Furthermore, the ^{13}C cross-polarization magic-angle spinning (CP/MAS) NMR spectroscopy revealed a signal at ~160 ppm, providing additional evidence for the formation of imine bonds (Figure S11). Additionally, thermogravimetric analysis (TGA) showcased the exceptional thermal stability of the synthesized COF samples, withstanding temperatures as high as 400-450°C under a N_2 atmosphere (Figures S12-S14).

The precise structural determination and characteristics of both isomers (JUC-620 and JUC-621) were confirmed through PXRD measurement and structural simulations using the Materials Studio software package (Figure 2a and 2b). Based on our previous finding,[15a] the obtained 3D COFs were topologically isomeric, with JUC-620 exhibiting a 7-fold interpenetrated **dia** topology and JUC-621 featuring a 5-fold interpenetrated **qtz** topology (Figure 2c and 2d). It is noteworthy that JUC-620 is overlapped (AA-stacking), whereas JUC-621 adopts a staggered (AB-stacking) arrangement along the *c*-axis. The simulated PXRD patterns were in strong agreement with the experimental results, demonstrating the high crystallinity of both COFs. The PXRD patterns for BCTB–PD, JUC-655, and JUC-656 displayed the first and most intense peaks at 3.28˚, 2.91˚, and 2.75˚, respectively, corresponding to the strong reflection from (110) planes (Figure 2e). Additionally, moderate peaks attributed to the reflection from (020), (200), (220), (320), and (330) planes were evident on the PXRD patterns. Following a geometrical energy minimization using Materials Studio, these COFs exhibited good agreement with the simulated PXRD pattern generated from the slipped AA stacking models with **sql** topology (Figure S15). Similarly, the PXRD analyses of PyTA-BC-Ph and JUC-557 revealed intense peaks, indicating high crystallinity and a close match with the simulated ones predicted by the AA-stacking mode with **sql** net (Figures 2f and S15). The Pawley refinement also demonstrated good consistency with the experimental PXRD patterns. All of these COFs were easily and successfully obtained with excellent crystallinity. It is important to note that reversible crystal structure transformations between solvated COFs and activated COFs were observed in JUC-620 with **dia** net, as well as in BCTB–PD, JUC-655, and JUC-656, where the peak shape changed and the position shifted,

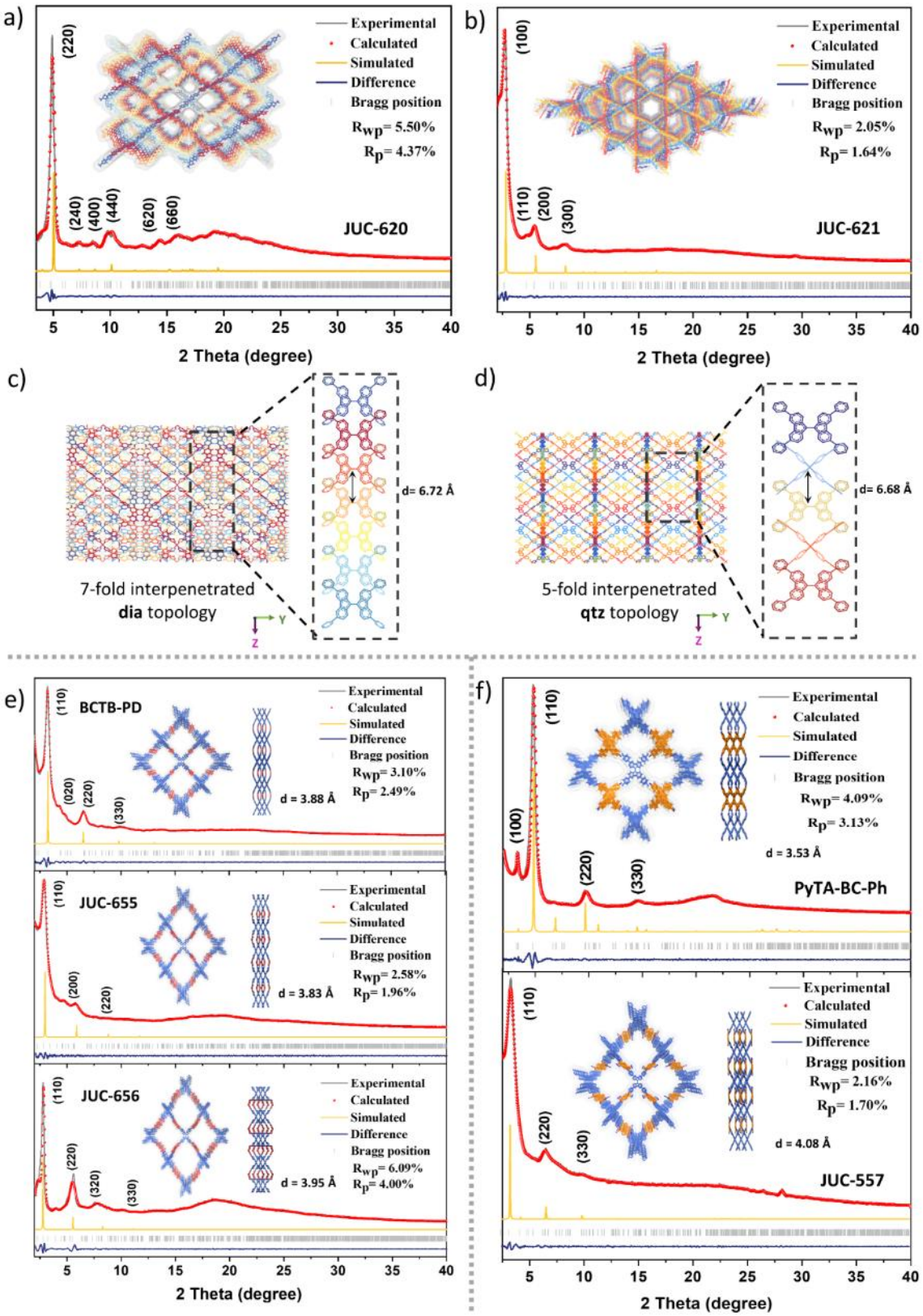

Figure 2. PXRD patterns of (a) JUC-620 based on 7-fold interpenetrated **dia** topology with AA stacking (c) and (b) JUC-621 based on 5-fold interpenetrated **qtz** topology with AB stacking (d). PXRD patterns of (e) BCTB-PD, JUC-655 and JUC-656, and (f) PyTA-BC-Ph and JUC-557. The inserted parts represent the corresponding porous structures of COFs.

indicating the flexibility of the frameworks (Figure S16).[19] The relative dynamics in these COFs differed notably from their counterparts (Figure S17), potentially leading to different piezochromic behaviors under hydrostatic pressure.

Nitrogen adsorption-desorption experiments at 77 K were conducted to assess the porosity of the COF samples, as shown in Figures S18-S24. The majority of the samples exhibited a reversible type-I isotherm, indicative of microporous structures, with the exception of JUC-621, which displayed a type-IV

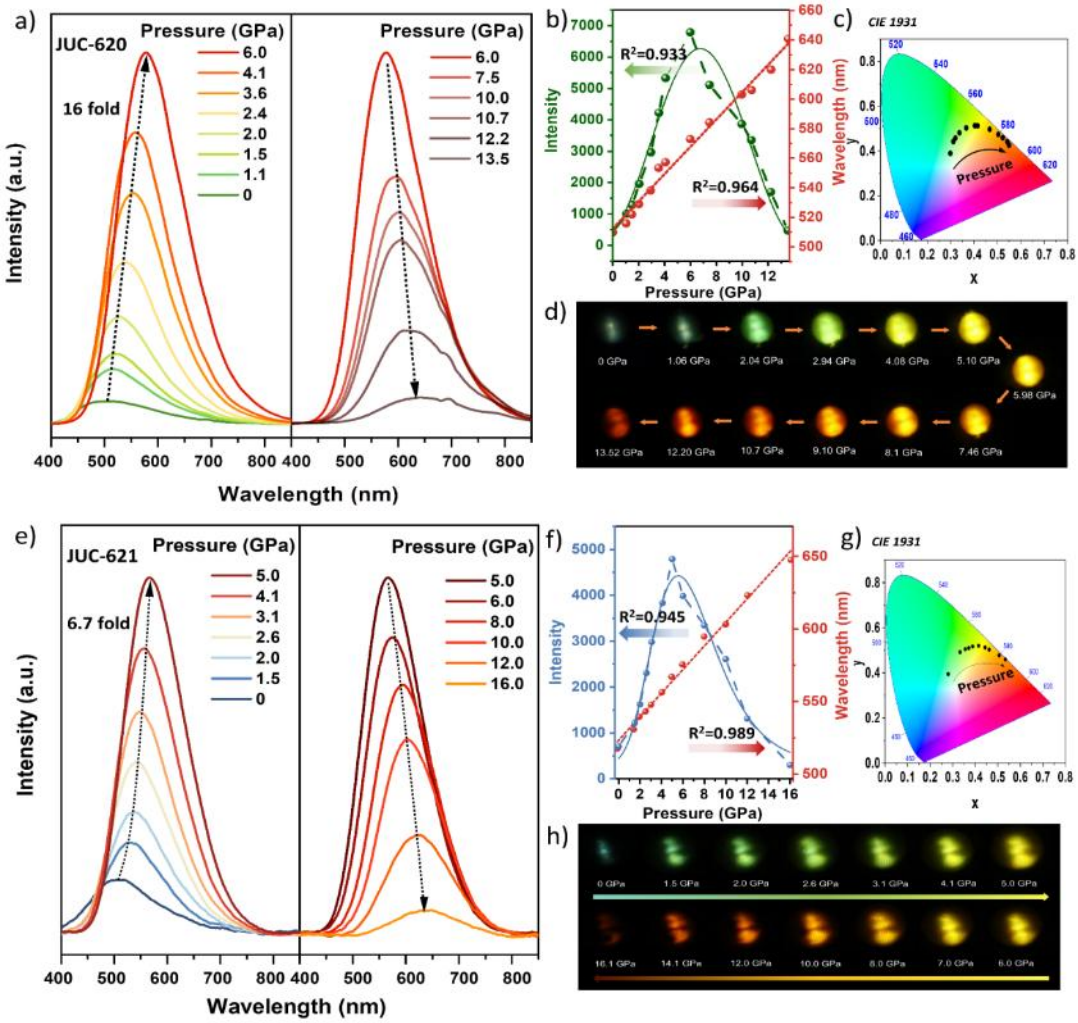

Figure 3. Fluorescence spectra and intensity-wavelength plots with corresponding chromaticity coordinates and photographs under UV irradiation (λ_{ex} = 355 nm) of (a–d) JUC-620 and (e–h) JUC-621 at various pressures from 1 atm (101 kPa) to 13.5 GPa and 16 GPa, respectively.

isotherm with a second step at P/P_0 = 0.2, a characteristic feature of mesoporous materials. Based on the N_2 adsorption isotherms, the corresponding Brunauer-Emmett-Teller (BET) surface areas of the COFs were determined to be 1120 $m^2\ g^{-1}$ for JUC-620, 1818 $m^2\ g^{-1}$ for JUC-621, 1880 $m^2\ g^{-1}$ for PyTA-BC-Ph, and 848 $m^2\ g^{-1}$ for JUC-557. The pore-size distribution was calculated using nonlocal density functional theory (NLDFT, Figures S18-S24). JUC-621 exhibited mesoporous channels with a size of 23 Å, while JUC-620, JUC-557, and PyTA-BC-Ph were found to be microporous materials with pore sizes of 12 Å, 18 Å, and 19 Å, respectively, consistent with previous reports. For BCTB–PD, JUC-655, and JUC-656, the BET surface areas were measured to be 2266 $m^2\ g^{-1}$, 1588 $m^2\ g^{-1}$, and 380 $m^2\ g^{-1}$, with pore size distributions of 16 Å, 21 Å, and 18 Å, respectively. The lower N_2 adsorption capacity of JUC-656 can be attributed to the contraction of its more flexible framework with a longer linker.

The photophysical properties of the COFs and corresponding monomers under atmospheric pressure were investigated using ultraviolet-visible (UV-Vis) absorption and photoluminescence (PL) spectroscopies. As depicted in Figure S25, the solid samples of the BCTB-4CHO compound showed a maximum absorption peak (λ_{abs}) at 367 nm, while the λ_{abs} of JUC-620 and JUC-621 further shifted bathochromically to 396 nm and 403 nm, respectively. Upon excitation, BCTB-4CHO emitted blue luminescence with peak maxima (λ_{em}) at 447 nm, and the red-shifted λ_{em} was also observed in the crystalline JUC-620 (464 nm) and JUC-621 (467 nm). For aromatic diamines linked COFs, the obtained samples displayed a broad absorption band in the 400−414 nm range, with emission maxima occurring at 480−497 nm. Similarly, redder absorption and emission can be observed in PyTA-BC-Ph and JUC-557 with λ_{em} of 518 nm and 552 nm, respectively. Notably, the 2D COFs demonstrated a gradual red-shift in absorption and emission compared to the 3D COFs, which is closely associated with the shorter layer spacing and stronger interactions in the 2D framework. Furthermore, arranging pyrene and olefin (C=C) into well-defined 2D COFs increases the effectiveness of conjugations between monomer units, leading to further red-shifts in absorption and emission.

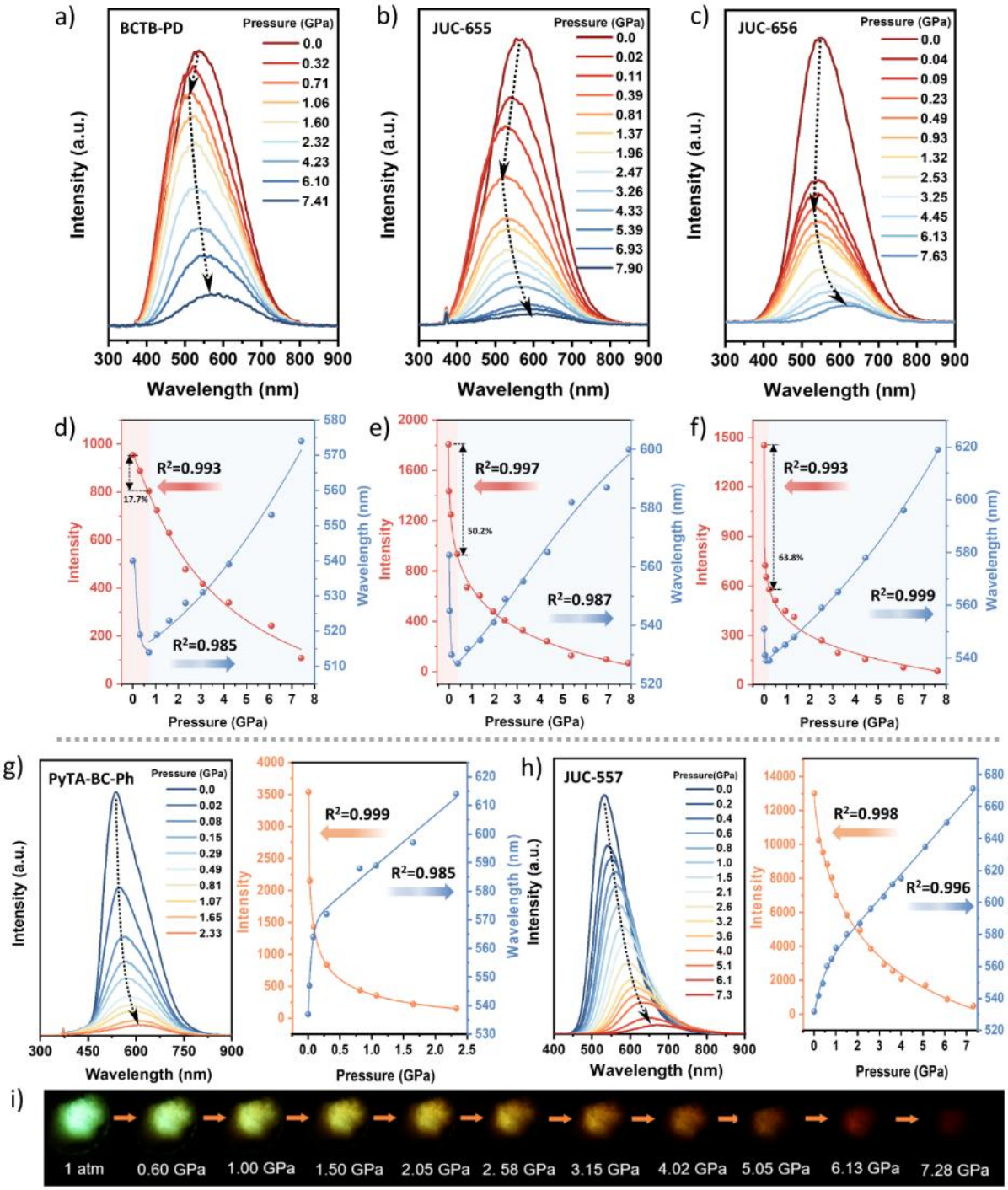

Figure 4. Fluorescence spectra and intensity-wavelength plots of (a,d) BCTB-PD, (b,e) JUC-655, (c,f) JUC-656, (g) PyTA-BC-Ph, and (h) JUC-557 at various pressures with 355 nm laser. (i) PL photograph of JUC-557 under high pressure.

It has been reported that herron-shaped carbazole small molecules tend to flatten after pressure treatment, showing an obvious PIEE phenomenon.[6a] Therefore, the pressure-modulated emission properties of bicarbazole-based COFs with different topologies, dimensions, and linkages can be expected through the DAC technique. Intriguingly, 3D bicarbazole-based COFs demonstrated a pronounced and efficient PIEE phenomenon. In the case of JUC-620, as the pressure increased from 1 atm to 6 GPa, the COF exhibited a gradual red-shift in emission with $\Delta\lambda_{em}$ of 63 nm, and the fluorescence intensity displayed a significant increasing trend, transitioning from weak grass-green to bright yellow (Figure 3a and 3d). The maximum PL intensity at 6 GPa was approximately 16-fold higher than the initial state. Upon further compression, the emission intensity of JUC-620 gradually decreased, and the wavelength continuously red-shifted until the pressure reached 13.5 GPa, at which point the intensity became relatively featureless, with a total shift of 134 nm (Figure 3b). The chromaticity coordinates of PL upon compression from 1 atm to 13.5 GPa are illustrated in Figure 3c. Notably, this marks the first instance in COFs where such a material exhibits unusual PIEE behavior, a rarity even in crystalline porous materials. The 16-fold increment surpasses the PIEE behavior reported in CPMs and most organic small molecules thus far (Table S1), such as

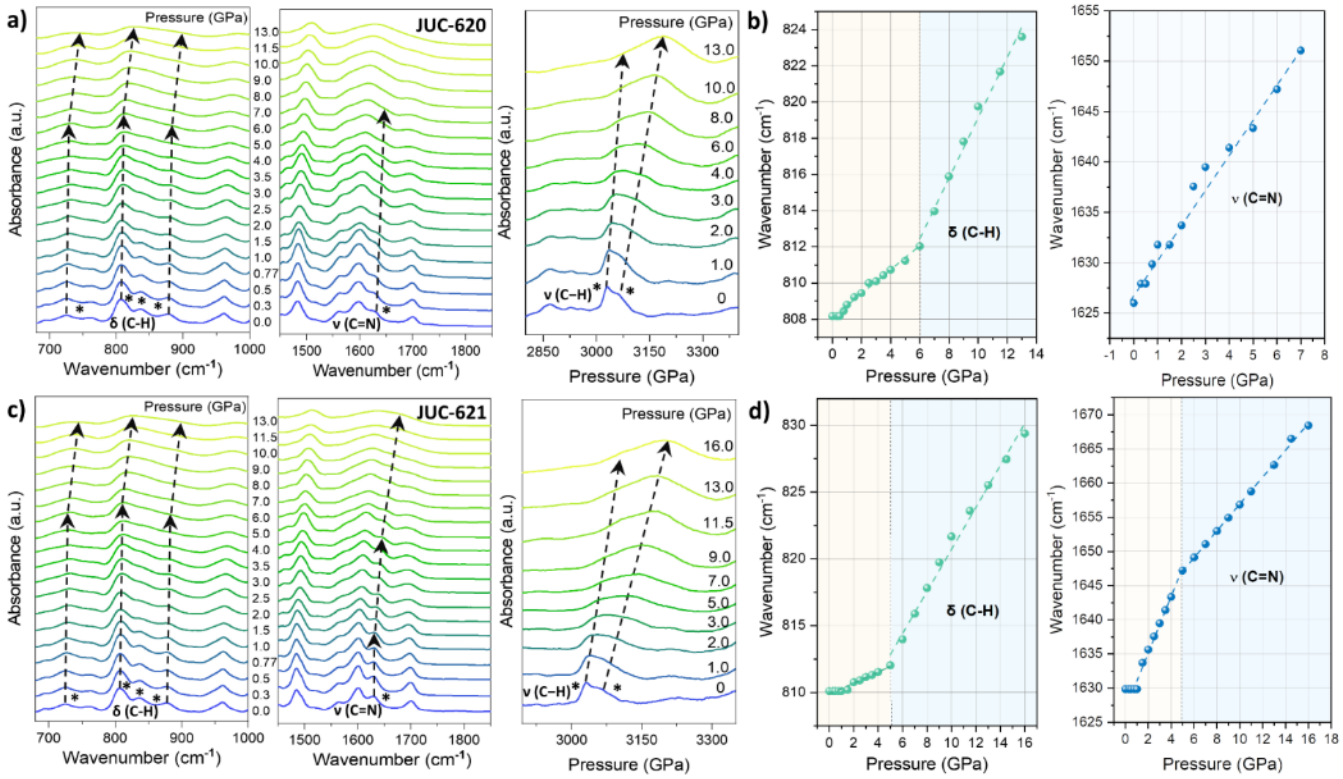

Figure 5. IR spectra of a) JUC-620 at the range of 0–13 GPa and c) JUC-621 at the range of 0–16 GPa. High-pressure IR spectra of b) JUC-620 and d) JUC-621 in the region of δ(C−H) and ν(C=N) vibration modes.

small molecule carbazole with a one-time increment,[6a] the classic chromophore tetraphenylethene with a 3-fold increment,[20] and the polycyclic aromatic hydrocarbon triphenylene with a 7.5-fold increment.[21] In addition to its excellent PIEE performance, JUC-620 also displayed high-contrast emission and a substantial red-shifted emission ($\Delta\lambda_{em}$ = 134 nm). These results indicate that COF materials offer significant advantages in piezochromism.

Motivated by the PIEE properties observed in JUC-620 with a **dia** net, we anticipated that JUC-621, with a **qtz** net as a topological isomer, would also exhibit unique piezochromism. Consequently, the PL intensity of JUC-621 increased by 6.7 times from 1 atm to 5 GPa, accompanied by a red-shift in emission of 50 nm. With further compression, the PL intensity gradually decreased and disappeared at 16 GPa, resulting in a total shift of 134 nm, similar to JUC-620 (Figure 3e and 3f). A series of optical photographs clearly illustrate the evolving trend of JUC-621: transitioning from weak green to bright yellow and finally to weak red (Figure 3h). Additionally, the chromaticity coordinates of JUC-621 during continuous compression were recorded (Figure 3g). Evidently, isomers with the same chemical composition but different topological structures exhibit similar PIEE phenomena during the compression process, with differences primarily in the enhancement multiple and the pressure at maximum fluorescence. Furthermore, upon decompression, the PL spectra of these COFs essentially returned to their original position, although the intensity could not maintain the maximum value (Figures S26 and S27). Moreover, unlike COFs, the emission intensity of the monomer (BCTB-4CHO) rapidly decreased with a continuous red-shift of the emission band and essentially lost its original fluorescence upon decompression (Figure S28), demonstrating that organic monomer did not influence the fluorescence enhancement of COFs through pressure treatment.

We hypothesize that the fluorescence enhancement is associated with the loose skeleton and relatively long distances between the penetration layers (6.7 Å) of 3D COFs, where greatly reduced distance and enhanced interactions are shown upon pressure. With these considerations in mind, we investigated the piezochromism of three imine-linked 2D COFs, namely BCTB–PD, JUC-655, and JUC-656, characterized by a more compact spacing of 3.8 Å between adjacent layers with slipped AA stacking models (Figure 2e). As anticipated, these bicarbazole-based 2D COFs did not display PIEE phenomena but exhibited a gradual decrease in fluorescence intensity with a red-shifted wavelength within a certain pressure range (Figure 4a-4c). The optical micrographs and chromaticity coordinates of the COFs clearly illustrate the changes in emission brightness and color (Figures S29-S31). Notably, a blue-shifted and weakened emission was observed in these three COFs at the onset of pressure, with BCTB–PD quenched by 17.7% at 0.7 GPa, JUC-655 quenched by 50.2% at 0.39 GPa, and JUC-656 quenched by 63.8% at 0.23 GPa (Figure 4d-4f). Only a very limited number of instances of blue-shifted emission have been reported in organic piezochromic materials (Table S2).[9c, 22] This blue-shift and weakened emission of COFs can be attributed to the pressure sensitivity of the flexible chain with imine linkage, where pressure intensified the vibration of imine and inhibited the energy transfer process, leading to fluorescence weakening during initial compression.[7a, 9c] Furthermore, it is evident that the fluorescence intensity decreased rapidly with increasing side chain length. This can be rationalized by the fact that as the length of the flexible side chain increases, the COFs become more fragile due to the large void space and the absence of π-π packing, resulting in weak resistance to pressure.[23] Meanwhile,

during the subsequent decompression process, the fluorescence of these COFs was reactivated, albeit with some intensity loss (Figure S32).

Furthermore, to provide a comparison, we introduced more rigidity and conjugation in PyTA-BC-Ph and JUC-557, and studied the piezochromism of these COFs. As depicted in Figure 4g and 4h, both COFs displayed red-shifted fluorescence emission and a gradual decrease in intensity, accompanied by changes in emission color and brightness (Figures 4i and S29). It is evident that the eclipsed interlayer packing aligns pyrene and olefin in the same direction, thereby intensifying the π-π stacking interaction between the 2D layered structures, leading to immediate fluorescence quenching.[24] Subsequently, after pressure release, neither of the two COFs could return to their initial state and exhibited reduced fluorescence (Figure S32d and S32e).

To investigate the operational mechanism of PIEE in 3D COFs, the structural parameters and piezochromism of the seven COFs were presented in Table S3. While it is challenging to make generalizations based on the dihedral angles of bicarbazole, it is possible to establish a correlation between the interlayer spacing of COFs and their piezochromism behavior, thus confirming our hypothesis that the enhanced fluorescence is linked to the layer spacing. Consequently, high-pressure in situ FT-IR spectra of the two 3D COFs were recorded in a DAC. As shown in Figure 5a and 5c, the bands within the range of 700-900 cm^{-1} were attributed to the deformation vibration of C–H bonds (δ(C-H)). As pressure increased, the δ(C-H) of both COFs showed minimal shifts within the pressure range that enhanced fluorescence. For instance, the IR absorption peaks at 810 cm^{-1} exhibited shifts of 4 cm^{-1} for JUC-620 at 6 GPa and 2 cm^{-1} for JUC-621 at 5 GPa, respectively (Figure 5b and 5d). This suggested the development of numerous complex intramolecular interactions within the framework, which limited the deformation vibration of C-H bonds, in turn, leading to a noticeable increase in fluorescence. However, beyond 6 GPa or 5 GPa, the IR absorption peaks of δ(C-H) shifted significantly to higher wavenumbers, indicating the shorter chemical bonds and higher vibration frequencies, which resulted in energy dissipation and then fluorescence quenching. The band at 1624 cm^{-1} can be identified as the stretching vibration of C=N (ν(C=N)), which is characteristic of the imine bonds. Upon applying pressure from 0 to 1 GPa, the IR absorption peaks of ν(C=N) in JUC-620 experienced a blue-shift of 6 cm^{-1}, while the band of JUC-621 remained unchanged (Figure 5b and 5d). This demonstrates that flexible frameworks with **dia** topology are more readily activated by pressure compared to the relatively rigid ones with **qtz** topology. With increasing pressure, the imine stretching vibration peaks of JUC-620 blue-shifted at a rate of 3.57 cm^{-1}/GPa, while JUC-621 exhibited a discontinuous change of 4.3 cm^{-1}/GPa at 1-5 GPa and 1.93 cm^{-1}/GPa at 5-16 GPa, suggesting that the vibration of the imine bonds was gradually constrained after 5 GPa due to the reduced distance at higher pressure. At the same time, the relative intensity of the IR absorption peaks of ν(C-H) (3030 cm^{-1} and 3060 cm^{-1}) changed due to the emergence of numerous newly formed C-H...C and C-H…π interactions within reduced layer spacing, further inhibiting the entire framework's vibration (Figure S33). In comparison to JUC-621, the higher pressure and stronger emission increment of JUC-620 may be attributed to its relatively flexible framework and greater interlayer interactions under pressure. Upon surpassing the maximum pressure-induced fluorescence, the IR vibration peaks of JUC-620 and JUC-621 continued to shift towards higher wavenumbers where the intensified π–π interactions and greater energy dissipation resulted in fluorescence quenching.

Overall, combined with the structure features and emission spectra of COFs, the direct evidence from IR collectively demonstrates that the PIEE of 3D COFs is associated with reduced distances and enhanced interactions between layers within the framework, while emission quenching is attributed to heightened energy dissipation and π–π interactions at higher pressure. This indicates that the relatively loose framework enables 3D COFs to more easily adjust their structures under high pressure, effectively enhancing emission efficiency, while the tight stack of 2D COFs is more likely to cause fluorescence quenching due to the amplified π–π interactions under high pressure. Furthermore, both 2D and 3D COFs, particularly those with flexible frameworks containing imine bonds, exhibit susceptibility to pressure, leading to structural and spectral alterations. Notably, imine vibrations result in rare blue-shifted emissions in the case of flexible 2D COFs. It is imperative to acknowledge that COFs with extensive conjugation are more prone to fluorescence quenching and display a continuous red shift due to significantly intensified π–π interactions.

Conclusion

In summary, this study elucidates the influence of various connections, orientations, and alignments of COFs on their performance, which arises from differences in dimensions, topologies, and linkages. As a potent tool, pressure can effectively modulate the aforementioned factors and emission properties in 2D and 3D bicarbazole-based COFs. Specifically, two topological isomers of 3D COFs demonstrate superior PIEE phenomena, exhibiting a 16-fold enhancement, surpassing reported CPMs and most organic small molecules with PIEE behavior. For comparison, three 2D COFs with flexible frameworks exhibit blue-shifted emission, a rarity in piezochromic materials. Furthermore, two 2D COFs with greater rigidity and conjugation display red-shifted and reduced emission. When considered alongside their respective structural and emissionl characteristics, as well as in situ FT-IR characterization, the diverse piezochromic behaviors can be attributed to variations in layer spacing and interactions under hydrostatic pressure. This research not only offers a fresh perspective on piezochromic COFs but also furnishes valuable insights into the relationship between microstructures and properties. Future work will continue to explore and focus on PIEE and the interception of high-pressure states.

Acknowledgements

This work was supported by National Key R&D Program of China (2022YFB3704900 and 2021YFF0500500), National Natural Science Foundation of China (22025504, 21621001, and 21390394), '111 Center' (BP0719036 and B17020), China Postdoctoral Science Foundation (2020TQ0118 and 2020M681034), and the program for JLU Science and

Technology Innovative Research Team. V.V., Q.F. and S.Q. acknowledge the collaboration in the framework of China-French joint laboratory "Zeolites".

Keywords: covalent organic frameworks • fluorescence • piezochromic behavior • pressure-induced emission enhancement • blue-shift

[1] a) A. Li, S. Xu, C. Bi, Y. Geng, H. Cui, W. Xu, *Mater. Chem. Front.* **2021**, *5*, 2588-2606; b) D. Zhao, M. Wang, G. Xiao, B. Zou, *J. Phys. Chem. Lett.* **2020**, *11*, 7297-7306.

[2] a) Y. Sagara, S. Yamane, M. Mitani, C. Weder, T. Kato, *Adv. Mater.* **2016**, *28*, 1073-1095; b) Z. Ma, G. Xiao, B. Zou, *Sci. Bull.* **2023**, *68*, 1588-1590.

[3] a) Q. Qi, J. Qian, X. Tan, J. Zhang, L. Wang, B. Xu, B. Zou, W. Tian, *Adv. Funct. Mater.* **2015**, *25*, 4005-4010; b) L. Wang, K.-Q. Ye, H.-Y. Zhang, *Chin Chem Lett.* **2016**, *27*, 1367-1375; c) Z. Yang, Z. Fu, H. Liu, M. Wu, N. Li, K. Wang, S.-T. Zhang, B. Zou, B. Yang, *Chem. Sci.* **2023**.

[4] a) Y. Shi, Z. Ma, D. Zhao, Y. Chen, Y. Cao, K. Wang, G. Xiao, B. Zou, *J. Am. Chem. Soc.* **2019**, *141*, 6504-6508; b) Y. Fang, L. Zhang, Y. Yu, X. Yang, K. Wang, B. Zou, *CCS Chem.* **2021**, *3*, 2203-2210.

[5] a) A. Sussardi, C. L. Hobday, R. J. Marshall, R. S. Forgan, A. C. Jones, S. A. Moggach, *Angew. Chem. Int. Ed.* **2020**, *59*, 8118-8122; b) X. Guo, N. Zhu, S. P. Wang, G. Li, F. Q. Bai, Y. Li, Y. Han, B. Zou, X. B. Chen, Z. Shi, S. Feng, *Angew. Chem. Int. Ed.* **2020**, *59*, 19716-19721; c) C.-X. Chen, Z.-W. Wei, Y.-N. Fan, P.-Y. Su, Y.-Y. Ai, Q.-F. Qiu, K. Wu, S.-Y. Yin, M. Pan, C.-Y. Su, *Chem.* **2018**, *4*, 2658-2669.

[6] a) Y. Gu, K. Wang, Y. Dai, G. Xiao, Y. Ma, Y. Qiao, B. Zou, *J. Phys. Chem. Lett.* **2017**, *8*, 4191-4196; b) Y. Gu, H. Liu, R. Qiu, Z. Liu, C. Wang, T. Katsura, H. Zhang, M. Wu, M. Yao, H. Zheng, K. Li, Y. Wang, K. Wang, B. Yang, Y. Ma, B. Zou, *J. Phys. Chem. Lett.* **2019**, *10*, 5557-5562; c) Z. Fu, H. Liu, J. Zhao, X. Zhang, X. Zheng, B. Yang, X. Yang, K. Wang, B. Zou, *J. Mater. Chem. C.* **2021**, *9*, 14578-14582.

[7] a) J. Zou, Y. Fang, Y. Shen, Y. Xia, K. Wang, C. Zhang, Y. Zhang, *Angew. Chem. Int. Ed.* **2022**, *61*, e202207426; b) C. Liu, G. Xiao, M. Yang, B. Zou, Z.-L. Zhang, D.-W. Pang, *Angew. Chem. Int. Ed.* **2018**, *57*, 1893-1897.

[8] Y. Fang, T. Shao, L. Zhang, L. Sui, G. Wu, K. Yuan, K. Wang, B. Zou, *J. Am. Chem. Soc.* **2021**, *1*, 459-466.

[9] a) K. Nagura, S. Saito, H. Yusa, H. Yamawaki, H. Fujihisa, H. Sato, Y. Shimoikeda, S. Yamaguchi, *J. Am. Chem. Soc.* **2013**, *135*, 10322-10325; b) S. Zhang, Y. Dai, S. Luo, Y. Gao, N. Gao, K. Wang, B. Zou, B. Yang, Y. Ma, *Adv. Funct. Mater.* **2017**, *27*, 1602276; c) H. Liu, Y. Gu, Y. Dai, K. Wang, S. Zhang, G. Chen, B. Zou, B. Yang, *J. Am. Chem. Soc.* **2020**, *142*, 1153-1158.

[10] a) X. Yin, C. Zhai, S. Hu, L. Yue, T. Xu, Z. Yao, Q. Li, R. Liu, M. Yao, B. Sundqvist, B. Liu, *Chem. Sci.* **2023**, *14*, 1479-1484; b) X. Wang, C. Qi, Z. Fu, H. Zhang, J. Wang, H.-T. Feng, K. Wang, B. Zou, J. W. Y. Lam, B. Z. Tang, *Mater. Horizons.* **2021**, *8*, 630-638.

[11] a) A. P. Cote, A. I. Benin, N. W. Ockwig, M. O'Keeffe, A. J. Matzger, O. M. Yaghi, *Science.* **2005**, *310*, 1166-1170; b) H. M. El-Kaderi, J. R. Hunt, J. L. Mendoza-Cortes, A. P. Cote, R. E. Taylor, M. O'Keeffe, O. M. Yaghi, *Science.* **2007**, *316*, 268-272; c) X. Guan, F. Chen, Q. Fang, S. Qiu, *Chem. Soc. Rev.* **2020**, *49*, 1357-1384; d) S. Kandambeth, A. Mallick, B. Lukose, M. V. Mane, T. Heine, R. Banerjee, *J. Am. Chem. Soc.* **2012**, *134*, 19524-19527; e) S. Kandambeth, K. Dey, R. Banerjee, *J. Am. Chem. Soc.* **2019**, *141*, 1807-1822; f) R.-R. Liang, F.-Z. Cui, A. Ru-Han, Q.-Y. Qi, X. Zhao, *CCS Chem.* **2020**, *2*, 139-145; g) M. Li, J. Liu, Y. Li, G. Xing, X. Yu, C. Peng, L. Chen, *CCS Chem.* **2020**, *3*, 696-706; h) C. He, Q.-J. Wu, M.-J. Mao, Y.-H. Zou, B.-T. Liu, Y.-B. Huang, R. Cao, *CCS Chem.* **2020**, *3*, 2368-2380.

[12] a) W. K. Haug, E. M. Moscarello, E. R. Wolfson, P. L. McGrier, *Chem. Soc. Rev.* **2020**, *49*, 839-864; b) Y. Cheng, J. Xin, L. Xiao, X. Wang, X. Zhou, D. Li, B. Gui, J. Sun, C. Wang, *J. Am. Chem. Soc.* **2023**, *145*, 18737-18741; c) L. Zhang, L. Yi, Z.-J. Sun, H. Deng, *Aggregate.* **2021**, *2*, e24.

[13] Z. Fu, K. Wang, B. Zou, *Chin Chem Lett.* **2019**, *30*, 1883-1894.

[14] J. Fang, Z. Fu, X. Chen, Y. Liu, F. Chen, Y. Wang, H. Li, Y. Yusran, K. Wang, V. Valtchev, S. Qiu, B. Zou, Q. Fang, *Angew. Chem. Int. Ed.* **2023**, *62*, e202304234.

[15] a) Y. Liu, J. Li, J. Lv, Z. Wang, J. Suo, J. Ren, J. Liu, D. Liu, Y. Wang, V. Valtchev, S. Qiu, D. Zhang, Q. Fang, *J. Am. Chem. Soc.* **2023**, *145*, 9679-9685; b) Y. Yuan, H. Huang, L. Chen, Y. Chen, *Macromolecules.* **2017**, *50*, 4993-5003.

[16] A. F. M. El-Mahdy, M.-Y. Lai, S.-W. Kuo, *J. Mater. Chem. C.* **2020**, *8*, 9520-9528.

[17] A. F. M. El-Mahdy, A. M. Elewa, S.-W. Huang, H.-H. Chou, S.-W. Kuo, *Adv. Opt. Mater.* **2020**, *8*, 2000641.

[18] Y. Liu, J. Ren, Y. Wang, X. Zhu, X. Guan, Z. Wang, Y. Zhou, L. Zhu, S. Qiu, S. Xiao, Q. Fang, *CCS Chem.* **2022**, *5*, 2033-2045.

[19] a) X. Liu, J. Li, B. Gui, G. Lin, Q. Fu, S. Yin, X. Liu, J. Sun, C. Wang, *J. Am. Chem. Soc.* **2021**, *143*, 2123-2129; b) Y. Chen, Z.-L. Shi, L. Wei, B. Zhou, J. Tan, H.-L. Zhou, Y.-B. Zhang, *J. Am. Chem. Soc.* **2019**, *141*, 3298-3303; c) S. Seth, S. Jhulki, *Mater. Horizons.* **2021**, *8*, 700-727.

[20] H. Yuan, K. Wang, K. Yang, B. Liu, B. Zou, *J. Phys. Chem. Lett.* **2014**, *5*, 2968-2973.

[21] A. Li, F. Li, Y. Chen, Y. Xie, X. Li, X. Liu, S. Xu, W. Xu, J. Wang, Z. Li, *ACS Mater. Lett.* **2022**, *4*, 2151-2158.

[22] a) J. Liu, G. Du, N. Liang, L. Yang, Y. Feng, Y. Chen, C.-J. Yao, *J. Mater. Chem. C.* **2023**, *11*, 8609-8615; b) J.-C. Yang, Z. Fu, H. Ma, T. Wang, Q. Li, K. Wang, L. Wu, P. Chen, H.-T. Feng, B. Z. Tang, *ACS Mater. Lett.* **2023**, *5*, 1441-1449.

[23] X. Guan, Q. Fang, Y. Yan, S. Qiu, *Acc. Chem. Res.* **2022**, *55*, 1912-1927.

[24] J. Han, Q. Zheng, C. Jin, S. Wang, Y. Liu, Y. Zhao, J. Zhu, *J. Phys. Chem. C.* **2022**, *126*, 16859-16866.

Entry for the Table of Contents

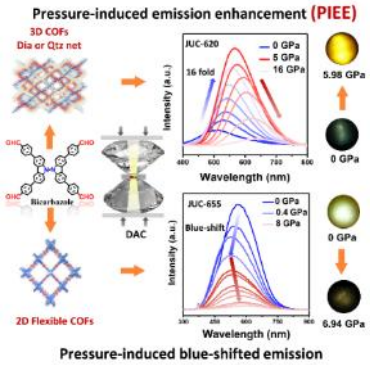

A range of 2D and 3D bicarbazole-based COFs with varying dimensions, topologies, and linkages were employed to systematically investigate their piezochromic behavior, revealing significant pressure-induced emission enhancement with an increase of 16-fold, as well as rare instances of blue-shifted emission.